

- with inductive strip—Planar circuit mounted in waveguide," *IEEE Trans. Microwave Theory Tech.*, vol. MTT-22, pp. 869–873, Oct. 1974.
- [24] E. S. Hensperger, "The design of multi-hole coupling arrays," *Microwave J.*, pp. 38–42, Aug. 1959.
- [25] T. Moreno, *Microwave Transmission Design Data*, New York: Dover Publications, 1958, pp. 176–178.
- [26] A. M. K. Saad and G. Begemann, "Electrical performance of fin-lines of various configurations," *Inst. Elec. Eng. (London), Journal on Microwaves, Optics, and Acoustics*, vol. 1, no. 2, pp. 81–88, Jan. 1977.
- [27] L. D. Cohen and P. J. Meier, "Advances in *E*-plane printed millimeter-wave circuits," in *IEEE Microwave Theory Tech. Symp. Digest*, pp. 27–29, June 1978.

# Hybrid Integrated Frequency Multipliers at 300 and 450 GHz

TOHRU TAKADA AND MASAHIRO HIRAYAMA

**Abstract**—300- and 450-GHz band doublers and triplers using thin-film integrated circuits have been developed. The multipliers are built with a GaAs honeycomb-type Schottky barrier diode designed to have a high cutoff frequency and transitions from microstrip to rectangular waveguides.

A 450-GHz band tripler delivered an output power of  $-11.2$  dBm with a corresponding conversion loss of 19.4 dB. The output power of the 300-GHz band doubler was  $-3.6$  dBm, and its minimum conversion loss was 10.7 dB.

The hybrid integrated frequency multipliers are useful as solid-state sources in the short-millimeter-wave and submillimeter-wave regions.

## I. INTRODUCTION

RECENTLY, there has been an increasing need for short-millimeter-wave and submillimeter-wave solid-state sources for use in radio astronomy, plasma diagnostics, spectroscopy, and target acquisition radars.

Frequency multipliers which are driven by IMPATT or Gunn oscillators are useful sources for these applications. Multipliers which deliver useful power levels have been developed up to the 300-GHz band [1]–[3]. However, in the higher frequency region, it is difficult to fabricate multipliers using conventional fabrication techniques because of the necessity of an extremely small tolerance. We have solved this difficulty in the 300- and 450-GHz regions using thin-film integrated-circuit techniques which were used for the millimeter-wave mixers up to the 230-GHz region [2], [4], and obtained good multiplication performances.

The hybrid integrated frequency multipliers have the following advantages: 1) an easy and high accuracy fabrication method in comparison with conventional

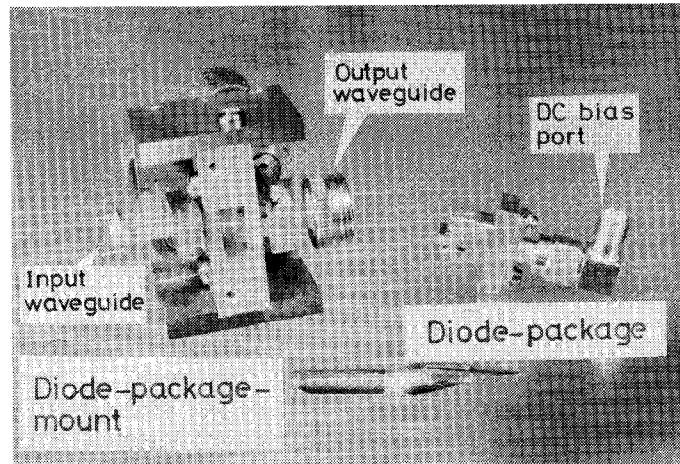


Fig. 1. Hybrid integrated frequency multiplier.

mechanical techniques, 2) possibilities of a compact and reproducible circuit design by using microstriplines, and 3) a possibility of realizing the devices at still higher frequencies [5], [6].

## II. DESIGN AND FABRICATION

A photograph of the hybrid integrated frequency multiplier is shown in Fig. 1. It consists of the following three main parts: 1) a diode-package mount, 2) a diode package, and 3) a diode chip.

### A. Diode-Package Mount

The diode-package mount consists of an input 150-GHz band waveguide (WR-6), an output 300-GHz band tapered waveguide (reduced WR-3), input and output short pistons, and micrometers for driving them. Input and output waveguides were realized as short as possible

Manuscript received October 12, 1977.

The authors are with the Musashino Electrical Communication Laboratory, NTT, Musashino, Japan.

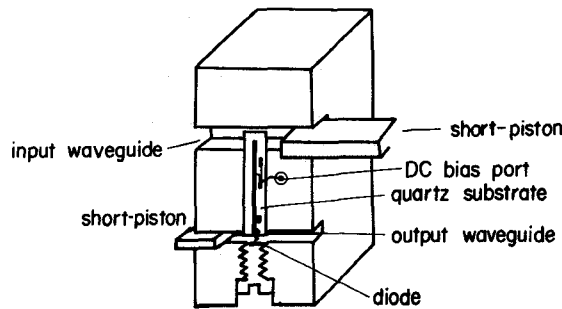


Fig. 2. Inner part of the diode package.

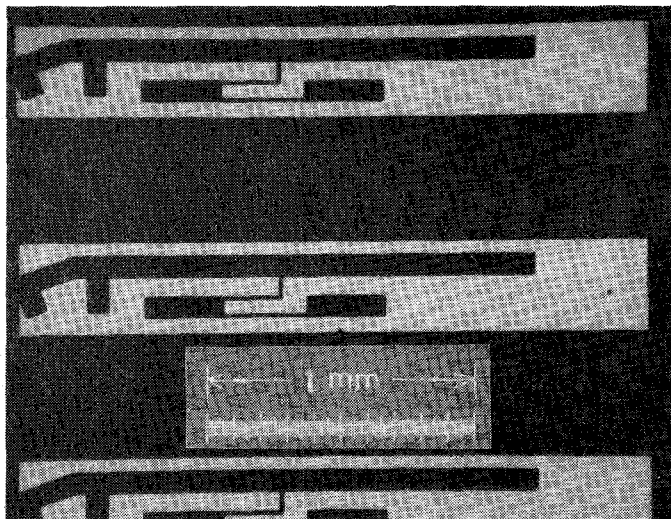


Fig. 3. Photograph of the thin-film integrated circuits before separating into individual substrates.

to reduce a propagation loss by developing a new mechanism to drive a short piston; an axis of the micrometer driving the short piston is crossed perpendicularly to the waveguide propagation axis as shown in Fig. 1.

#### B. Diode-Package

Fig. 2 shows the inner part of the diode package which consists of an input waveguide ( $1.651 \text{ mm} \times 0.825 \text{ mm}$ ), an output reduced height waveguide ( $0.864 \text{ mm} \times 0.200 \text{ mm}$ ), a thin-film integrated circuit whose photograph is shown in Fig. 3, a dc bias port, and a diode chip. Circuits needed for multiplication are integrated on the quartz substrate ( $0.34\text{-mm width, 2.3-mm length, 0.06-mm thickness}$ ) which is mounted on the ground plane of the microstrip enclosure by the resin Aron Alpha<sup>1</sup>. Since a cutoff frequency of the longitudinal-section-magnetic mode existing in the microstrip channel is  $371 \text{ GHz}$  [7] and a cutoff frequency of the lowest order transvers-electric-surface mode is  $750 \text{ GHz}$  [8], a  $150\text{-GHz}$  band fundamental wave and  $300\text{-GHz}$  band second harmonic wave propagate only with a dominant microstrip mode, pseudo TEM mode. Fig. 4 shows a top and cross-sectional view and design of the thin-film integrated circuit. The incoming  $150\text{-GHz}$  band wave from the input waveguide couples to the microstripline by

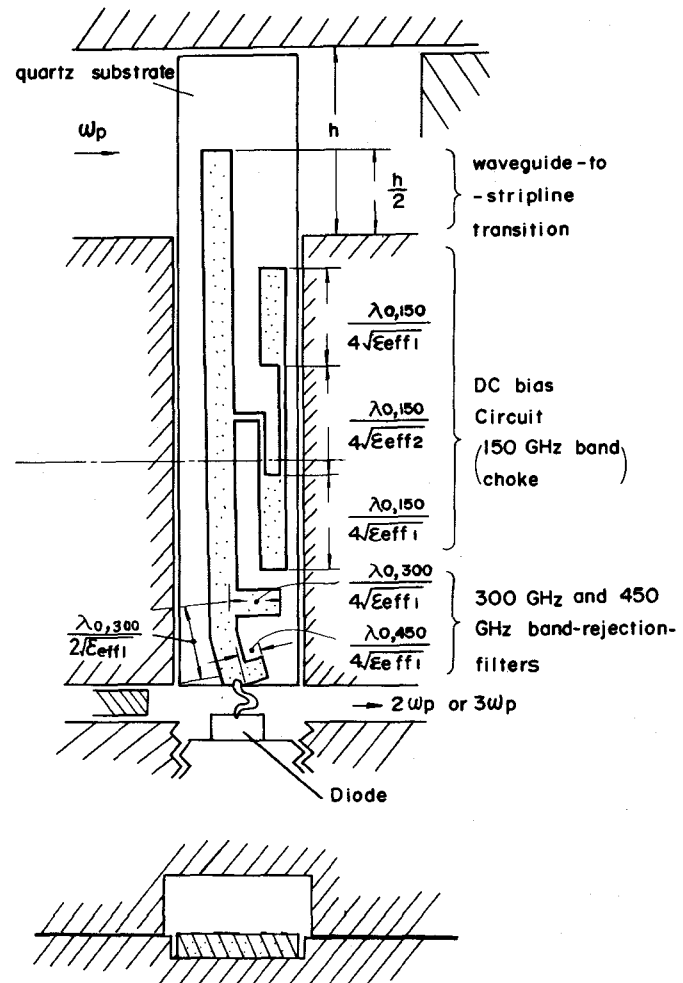


Fig. 4. Top and cross-sectional view and design of integrated circuit.

from the input waveguide couples to the microstripline by means of a probe. An optimum length of the probe is about a half of the waveguide height, which was experimentally determined from a scaling experiment at the  $10\text{-GHz}$  band. The  $150\text{-GHz}$  wave propagates in the microstripline and pumps the Schottky barrier diode, and then harmonic waves are generated. To prevent the propagation of the second and the third harmonics to the input port, band-rejection-filters which consist of quarter-wavelength shunt stubs are used. In order to reject the propagation of the input wave toward the dc bias port, quarter-wavelength high impedance lines and open-terminated low impedance lines at  $150 \text{ GHz}$  are fabricated. Effective dielectric constants for determining the length of each line were obtained from the Schneider's formula [9]. In the previous work on a  $230\text{-GHz}$  band multiplier [10], the internal impedance matching circuit was fabricated on a quartz substrate. However, in this experiment, the input circuit impedance is designed to be  $65 \Omega$  which is nearly equal to the diode input impedance without an internal matching circuit.

A Pt whisker ( $250 \mu\text{m}$  long,  $10\text{-}\mu\text{m}$  diameter) was thermocompression bonded to an end of the circuit pattern. As shown in Fig. 2, the dc bias port of the package was connected to a dc bias circuit pattern with a  $20\text{-}\mu\text{m}$

<sup>1</sup>The manufacturer is Toa Gosei Chemical Industry Company, Limited, 2-12-15, Shinbashi, Minato-ku, Tokyo, Japan.

diameter Au wire using an ultrasonic bonding technique. A diode chip was soldered on top of the screw and was inserted into the lower side of the output waveguide, and one of the honeycomb junction was connected to the whisker under a microscope.

The thin-film integrated circuits were fabricated by the following process, that is, evaporating of Cr (100 Å) and Au (500 Å) on the quartz substrate (10 mm × 10 mm), patterning of photo resist, selective electroplating of Au to a thickness of about 2 μm, removing of the photo-resist, chemical etching of Au and Cr layers, and cutting the substrate to separate each thin-film circuit plate. An Au layer with a thickness of 2 μm is needed for good bonding of the Pt whisker and Au wire to the conductor pattern. However, using the usual chemical photo-etching process, it is difficult to obtain the desired conductor pattern with such a thick Au layer because of undercutting owing to the etching process. We solved this problem using the above selective electroplating process in which the undercutting was about 0.1 μm and fabricated the smallest line width of 20 μm with an accuracy of less than 1 μm.

The input and output waveguides and microstrip enclosure were fabricated by shaving brass with a diamond bit. Since the skin depth in the metal is very small at submillimeter wavelengths (0.14 μm at 300 GHz for Au), the surface roughness of the waveguide wall should be made as small as possible. So, we tried this technique and got good surfaces as shown in Fig. 5.

### C. Diode Chip

GaAs honeycomb-type Schottky barrier diodes shown in Fig. 6 were used as a variable capacitance diode. A Ni-Au Schottky barrier was fabricated on an n-type epitaxial layer by electroplating [11]. A diameter of the junction, a carrier concentration, and a thickness of the epitaxial layer were designed according to the results of the following calculations of the cutoff frequency.

The cutoff frequency for a multiplier diode is expressed as follows [12]:

$$f_c = \frac{S_{\max} - S_{\min}}{2\pi R_s} \quad (1)$$

where  $S_{\max}$  and  $S_{\min}$  are the maximum and minimum values of elastance and  $R_s$  is the series resistance of the diode. If the diode junction is assumed to be fully pumped from the built in potential  $V_{bi}$  to the breakdown voltage  $V_B$ ,

$$f_c = 1/2\pi C_B (R_{\text{epi}} + R_{\text{sub}}) \quad (2)$$

where  $C_B$  is the junction capacitance at  $V_B$  and  $R_{\text{epi}}$  and  $R_{\text{sub}}$  are the resistance of the epitaxial layer and the substrate, respectively. We calculated  $f_c$  from (2) under the assumption that the epitaxial layer thickness was designed to be equal to the punch-through thickness at the breakdown voltage.

The calculated result of the cutoff frequency  $f_c$  versus carrier concentration of the epitaxial layer  $N_d$  is shown in Fig. 7. It is shown that the  $f_c$  increases as the junction

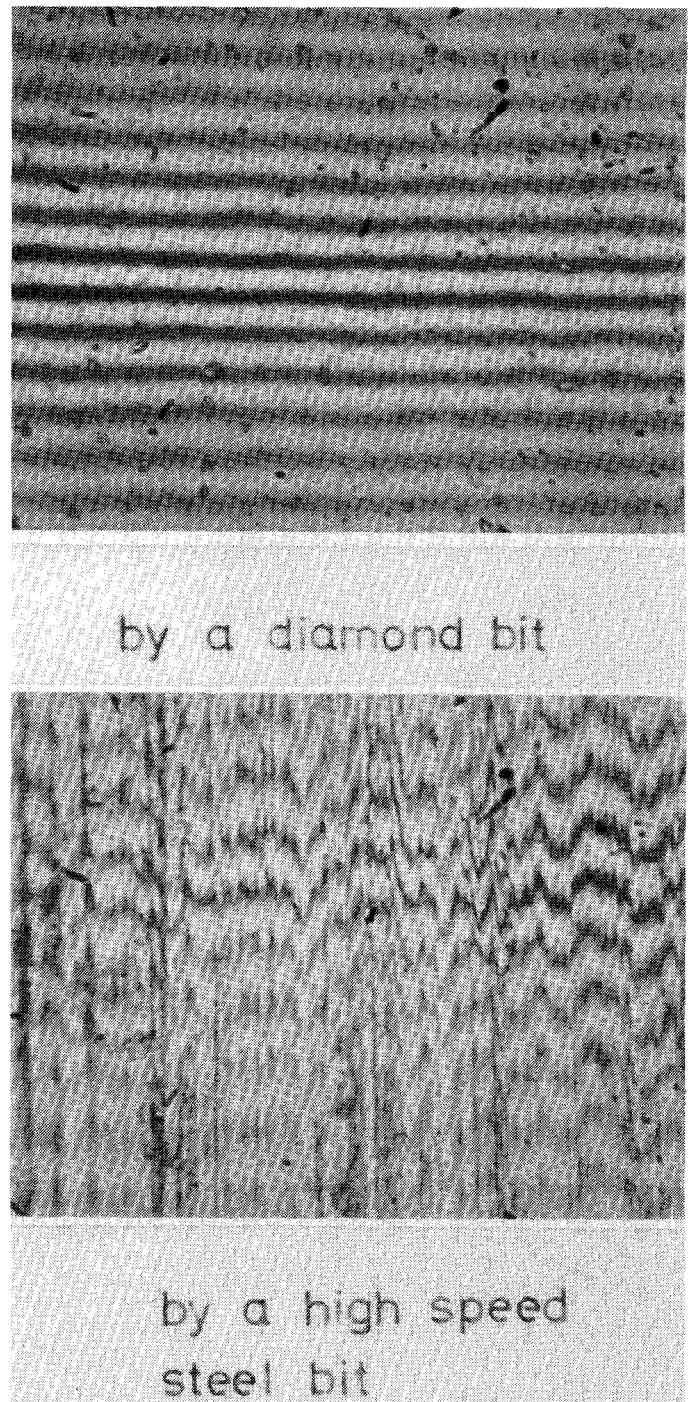


Fig. 5. Photographs of the brass surfaces using a diamond bit and a high speed steel bit by a interference microscope with a 1000× magnifications. An interval of the stripe is 2735 Å. The brass surface shaved by the diamond bit looks like a mirror with the naked eye.

diameter  $2r$  decreases, and there is an optimum  $N_d$  for each  $r$ . The reason is explained as follows. In the region of small  $r$  and low  $N_d$ ,  $f_c$  increases with  $N_d$  because the decrease of  $R_s$  is superior to the increase of  $C_B$ . On the other hand, in the region of large  $r$  and high  $N_d$ , since  $R_s$  is mostly dependent on  $R_{\text{sub}}$ ,  $f_c$  decreases owing to the increase of  $C_B$ .

In this experiment, two kinds of diodes with a junction diameter of 1.5 μm (No. 1) and 2.0 μm (No. 2) were used. The junction diameters were selected from a viewpoint of

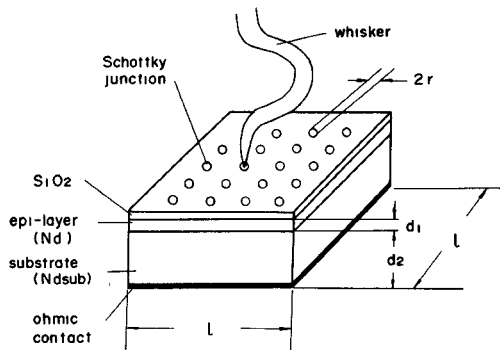


Fig. 6. GaAs honeycomb-type Schottky barrier diode, where,  $l$ ,  $d_2$ , and  $N_{d\text{sub}}$  are 150  $\mu\text{m}$ , 100  $\mu\text{m}$ , and  $2 \times 10^{18} \text{ cm}^{-3}$ , respectively.

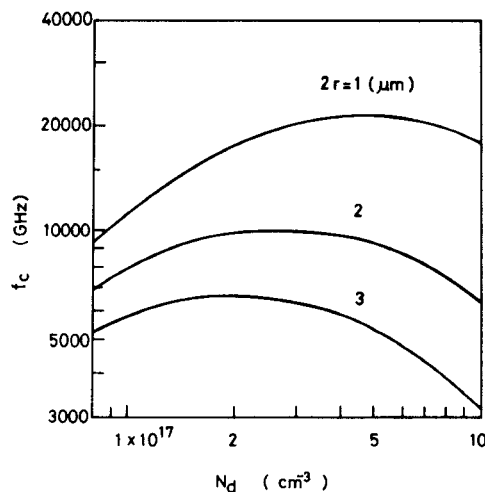


Fig. 7. Diode cutoff frequency versus carrier concentration of epitaxial layer with junction diameter as a parameter.

TABLE I  
DIODE PARAMETERS AND DC CHARACTERISTICS

type num- ber	diameter	carrier concent- ration of epi-layer	thickness of epi-layer	diode resistance (dc) $R_s$	break down voltage, $V_B$ (at 50 $\mu\text{A}$ )	ideality factor, $n$	junction capacitance of $V_B$ , $C_B$	cutoff frequency $f_c = 2\pi C_B R_s$
1	15 $\mu\text{m}$	$25 \times 10^{17}$	0.3 $\mu\text{m}$	41.0 $\Omega$	84 $\text{V}$	1.13	0.9 $\text{fF}$	4400 $\text{GHz}$
2	20	$25 \times 10^{17}$	0.15	150	47	1.17	2.4	4400

impedance matching which is extremely difficult at submillimeter wavelengths using external tuning components. The characteristic impedance of the waveguide whose height is reduced to 0.2 mm is 168–149  $\Omega$  for 300–450 GHz. On the other hand, the diode output impedances of the tripler using a No. 1 diode and the doubler using a No. 2 diode are 107 and 68  $\Omega$  [12], respectively, which are not so different from the characteristic impedances of the output waveguide. Input diode impedances of the tripler and doubler are calculated to be 85 and 45  $\Omega$  [12], respectively, which are nearly equal to the input circuit impedance. Table I shows the diode parameters and their dc characteristics. The  $C_B$  and  $f_c$  were calculated and others were measured values. The  $R_s$  includes the measured contact resistance, 7–10  $\Omega$ , between the barrier metal and the whisker.

### III. MEASUREMENT

A 150-GHz band klystron was used as an input source. The output power at 300 GHz was measured with a commercial thin-film thermocouple calibrated by a dry calorimeter. At 450 GHz, since commercial power meters were not available, the power was measured by using the Si point contact detector which was calibrated by the dry calorimeter. The sensitivity of the detector at 438.8 GHz was 13.3 V/W.

The output frequency in the 300- and 450-GHz band was calculated from the waveguide wavelength that was detected by the Si point contact diode with a movable back piston and was verified with cutoff waveguide test sections.

Tuning of the multiplier was made by adjusting the short pistons in the input and output waveguides and the dc bias voltage. For the tripler operation of the multiplier, a 350-GHz cutoff filter was connected after the output waveguide flange and a different tuning from the doubler operation was made.  $E$ - $H$  tuners were not used, because we experienced that they had large losses in the 230-GHz band [10].

### IV. RESULTS

#### A. 300-GHz Band Doubler

Experimental results of output power and conversion loss versus input power are shown in Fig. 8. A maximum output power of the doubler using a No. 1 diode was  $-3.6$  dBm at an input power level of 7.1 dBm, corresponding to a conversion loss of 10.7 dB. A maximum output power of the doubler using a No. 2 diode was the same level as the doubler using a No. 1 diode. We consider that since the conversion loss of the doubler No. 2 was not saturated, it can be expected to deliver larger output power and lower conversion loss if larger input power could be supplied.

Fig. 9 shows the output power as a function of diode dc bias voltage. The curves were measured, fixing the input and output short pistons after adjusting them at the optimum bias voltage. Since the curves of Fig. 9 are perfectly monotonic, spurious waves are not generated [13].

#### B. 450-GHz Band Tripler

The 450-GHz band tripler was measured using a No. 1 diode. The output power and conversion loss versus the input power is shown in Fig. 10. A maximum power of  $-11.2$  dBm, corresponding to a conversion loss of 19.4 dB was obtained. This is the highest power level obtained from a semiconductor device at the 450-GHz band up to date.

Fig. 11 shows the output power as a function of the diode dc bias voltage. It is inferred by the same reason as for the doubler that spurious waves are not generated.

### V. CONCLUSION

Hybrid integrated frequency doublers and triplers using GaAs Schottky barrier diodes have been developed in the 300- and 450-GHz bands. A 300-GHz band doubler de-

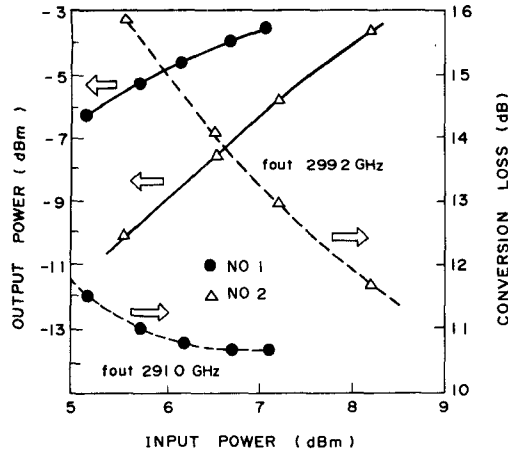


Fig. 8. Output power and conversion loss of 300-GHz band doubler.

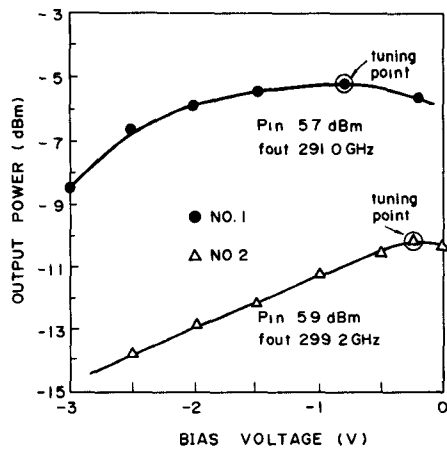


Fig. 9. Output power of 300-GHz doubler versus dc bias voltage.

livered the maximum power of  $-3.6$  dBm at an input power level of  $7.1$  dBm, corresponding to a conversion loss of  $10.7$  dB. A  $450$ -GHz band tripler delivered the maximum power of  $-11.2$  dBm, corresponding to a conversion loss of  $19.4$  dB.

The  $300$ -GHz band doubler will be used as a high efficiency local oscillator in semiconductor diode mixers and the  $450$ -GHz band tripler will be suitable for use as a local oscillator for a Josephson junction mixer which requires the relatively small local power of less than  $-20$  dBm for the submillimeter-wave region [14].

#### ACKNOWLEDGMENT

The authors wish to thank M. Ida and T. Yagasaki for advice and assistance of fabricating the diodes, M. Ohmori and T. Ishibashi for the useful suggestions, and M. Watanabe and M. Fujimoto for encouragement.

#### REFERENCES

- [1] L. D. Cohen, S. Nussbaum, E. Kraemer, J. Calviello, and J. Taub, "Varactor frequency doublers and triplers for the 200 to 300 GHz range," *IEEE-MTT-S Int. Microwave Symp. Technical Dig.*, 14-7 1100, pp. 274-276, May 1975.
- [2] G. T. Wrixon, "Low noise diodes and mixers for the 1-2 mm wavelength region," *IEEE Trans. Microwave Theory Tech.*, vol. MTT-22, p. 1163, Dec. 1974.
- [3] M. V. Schneider and G. T. Wrixon, "Development and testing of a receiver at 230 GHz," in *Proc. 1974 IEEE S-MTT Int. Microwave Symp. Technical Digest*, pp. 120-122, June 1974. (IEEE Catalog No. 74 CH 838-3 MTT.)
- [4] A. R. Kerr, R. J. Mattauch, and J. A. Grange, "A new mixer design for 140-220 GHz," *IEEE Trans. Microwave Theory Tech.*, vol. MTT-25, pp. 399-401, May 1977.
- [5] M. V. Schneider and W. W. Snell, Jr., "A scaled hybrid integrated multiplier from 10 to 30 GHz," *Bell Syst. Technical J.*, vol. 50, pp. 1933-1942, July-August 1971.
- [6] M. V. Schneider and W. W. Snell, Jr., "Hybrid integrated frequency multiplier from 10-30 GHz," *Proc. IEEE*, vol. 58, pp. 1402-1404, Sept. 1970.
- [7] M. V. Schneider, "Millimeter-wave integrated circuits," presented at *G-MTT Int. Microwave Symp.* 16-18, June 1973.
- [8] C. P. Hartwig, D. Masse, and A. P. Pucel, "Frequency dependent behavior of microstrip," in *1968 G-MTT Int. Microwave Symp. Digest*, (Detroit, MI, May 20-22), pp. 110-116, 1968.
- [9] M. V. Schneider, "Microstrip lines for microwave integrated circuits," *B.S.T.J.*, vol. 48, pp. 1421-1444, May-June 1969.
- [10] T. Takada and M. Hirayama, "Study of short millimeter wave doubler," *Paper Tech. Group on Microwaves*, IECE, Japan, MW 76-109, pp. 55-60, Dec. 1976.
- [11] Y. Sato, M. Uchida, K. Shimada, M. Ida, and T. Imai, "GaAs Schottky barrier diode, ECL-1314," *Review of Electrical Communication Laboratory*, vol. 18, no. 9-10, pp. 638-644, Sept.-Oct. 1970.
- [12] P. Jr. Penfield and R. P. Rafuse, *Varactor Applications*. M.I.T. Press, pp. 86, 331, and 351, 1962.
- [13] M. Hirayama, "100 and 150 GHz-band crossed-waveguide type diodes characteristics," *Trans. Int. Elec. Commun. Eng. Japan*, vol. 58-B, no. 7, pp. 345-352, 1975.
- [14] J. Edrich, "Results, potentials, and limitations of Josephson mixer receivers at millimeter and long submillimeter wavelengths," in *IEEE Dig. Submillimeter Cont.*, (San Juan, Puerto Rico, Dec. 6-10, 1976), pp. 181-182.

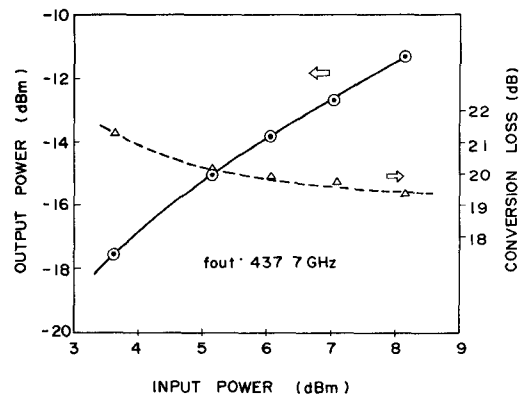


Fig. 10. Output power and conversion loss of 450-GHz band tripler.

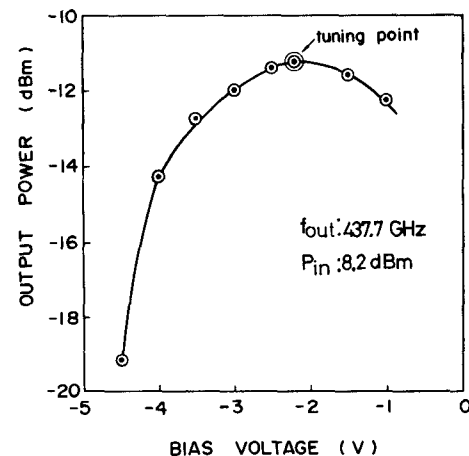


Fig. 11. Output power of 450-GHz tripler versus dc bias voltage.